Supplementary Information (SI) for Journal of Materials Chemistry C.
This journal is © The Royal Society of Chemistry 2024

Electronic Supplementary Information

for

Ultraviolet circularly polarized light detection based on chiral BN-anthracene derivatives

Wanhui Li,[a] Yi Zhang,[a] Kai-Yin Ren,[a] Cheng-Zhuo Du,[a] Ze-Fan Yao,[b] Jian Pei,[b] Xiao-Ye Wang*[a]

[a]State Key Laboratory of Elemento-Organic Chemistry, Frontiers Science Center for New Organic Matter, Haihe Laboratory of Sustainable Chemical Transformations, College of Chemistry, Nankai University, Tianjin 300071, China. E-mail: xiaoye.wang@nankai.edu.cn

[b]Beijing National Laboratory for Molecular Sciences (BNLMS), Key Laboratory of Bioorganic Chemistry and Molecular Engineering of Ministry of Education, Center of Soft Matter Science and Engineering, College of Chemistry and Molecular Engineering, Peking University, Beijing 100871, China.

Table of Contents

1. General Methods

Unless otherwise noted, all materials were purchased from commercial sources and all these chemicals were used as received without further purification. Anhydrous toluene, diethyl ether, and tetrahydrofuran (THF) were obtained from an Ultimate Solvent System 4S (USS-4S). Thin layer chromatography (TLC) was performed on silica gel with GF254 indicator. All yields given referred to isolated yields. Nuclear magnetic resonance (NMR) spectra were recorded on AVANCE 400 MHz Bruker spectrometers. Chemical shifts (δ) were reported in ppm. Coupling constants (J values) were reported in Hertz. ^{1}H NMR chemical shifts were referenced to $CHCl_3$ (7.260 ppm). ^{13}C NMR chemical shifts were referenced to $CDCl_3$ (77.00 ppm). High-resolution mass spectrometry (HRMS) was performed on a Bruker Solarix scimax MRMS by matrix-assisted laser desorption/ionization (MALDI). Optical microscope images were collected on a Nikon Eclipse LV150N Stand optical microscope. UV-vis absorption spectra were measured on an Analytikjena Specord 210 Plus UV-vis spectrometer. Fluorescence spectra were recorded on an Edinburgh FS5 Spectrofluorometer. Tapping-mode atomic force microscope (AFM) images were recorded using a Bruker Dimensional Icon AFM in air. Cyclic voltammograms (CV) were measured under an argon atmosphere on a CHI 620E electrochemical workstation. Circular dichroism (CD) spectra were collected on MOS-450 circular dichroism spectrometer. Theoretical calculations were performed using the Gaussian 09 software package.[1] All calculations were carried out using the density functional theory (DFT) method. The geometries were optimized at the B3LYP/6-31G(d) level.

2. Synthetic Procedures

(*R*)-/(*S*)-1-Bromo-4-(3,7-dimethyloctyl)benzene ((*R*)-/(*S*)-**1**)[2] and 2,7-dichloro-1,2,6,7-tetrahydrobenzo[1,2-*e*:4,5-*e*']bis([1,2]azaborinine) (**4**)[3] were synthesized according to reported procedures.

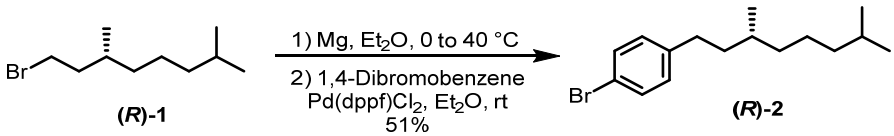

(*R*)-1-Bromo-4-(3,7-dimethyloctyl)benzene ((*R*)-2). A solution of (*R*)-**1** (3.32 g, 15.0 mmol) in 5 mL of diethyl ether under argon was added dropwise to a suspension of Mg (3.54 g, 149 mmol)

in 4 mL of diethyl ether at 0 °C. The mixture was refluxed at 40 °C for 1 h and then was cooled down to room temperature. The resulting Grignard reagent was added dropwise to a solution of 1,4-dibromobenzene (2.80 g, 12.0 mmol) and Pd(dppf)Cl_2 (436 mg, 0.596 mmol) in 9 mL of diethyl ether while the temperature was kept at 0 °C. The resulting mixture was allowed to warm to room temperature and stirred for 24 h. After completion of the reaction, water was slowly added to the mixture. The organic phase was separated, washed with water and dried over magnesium sulphate. The solvent was removed under reduced pressure, and the residue was purified by column chromatography over silica gel (eluent: petroleum ether) to give 1.80 g (51%) of (*R*)-**2** as a colourless liquid. ^{1}H NMR (400 MHz, $CDCl_3$, 298 K, ppm) δ 7.38 (d, J = 8.4 Hz, 2H), 7.05 (d, J = 8.4 Hz, 2H), 2.63-2.45 (m, 2H), 1.40-1.35 (m, 2H), 1.28-1.22 (m, 4H), 1.13-1.10 (m, 4H), 0.91 (d, J = 6.0 Hz, 3H), 0.83 (s, 6H).

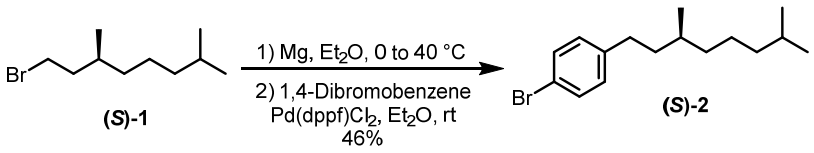

(*S*)-1-Bromo-4-(3,7-dimethyloctyl)benzene ((*S*)-2). Compound (*S*)-**2** was synthesized according to the same procedure as described above for the synthesis of (*R*)-**2** using (*S*)-**1** (5.53 g, 25.0 mmol), Mg (1.80 g, 75.0 mmol), 1,4-dibromobenzene (4.72 g, 20.0 mmol) and Pd(dppf)Cl_2 (732 mg, 1.00 mmol). After completion of the reaction, water was slowly added to the mixture. The organic phase was separated, washed with water and dried over magnesium sulphate. The solvent was removed under reduced pressure, and the residue was purified by column chromatography over silica gel (eluent: petroleum ether) to give 2.73 g (46%) of (*S*)-**2** as a colourless liquid. ^{1}H NMR (400 MHz, $CDCl_3$, 298 K, ppm) δ 7.38 (d, J = 8.4 Hz, 2H), 7.05 (d, J = 8.4 Hz, 2H), 2.63-2.45 (m, 2H), 1.40-1.35 (m, 2H), 1.28-1.22 (m, 4H), 1.13-1.10 (m, 4H), 0.91 (d, J = 6.0 Hz, 3H), 0.83 (s, 6H).

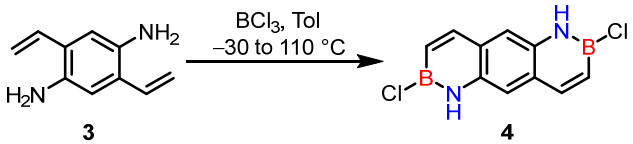

2,7-Dichloro-1,2,6,7-tetrahydrobenzo[1,2-*e*:4,5-*e*']bis([1,2]azaborinine) (4). To a Schlenk

tube under argon was added **3** (133 mg, 0.831 mmol) and dry toluene (20 mL). The resulting solution was cooled to –30 °C and BCl_3 (3.3 mL, 3.3 mmol, 1.0 M in CH_2Cl_2) was then added dropwise. After stirring at room temperature for 1 h, the mixture was stirred at 110 °C for 20 h. After cooling to room temperature, the solvent was removed under reduced pressure to give compound **4** as a white solid, which was directly used for the next step without further purification because of its high air sensitivity.

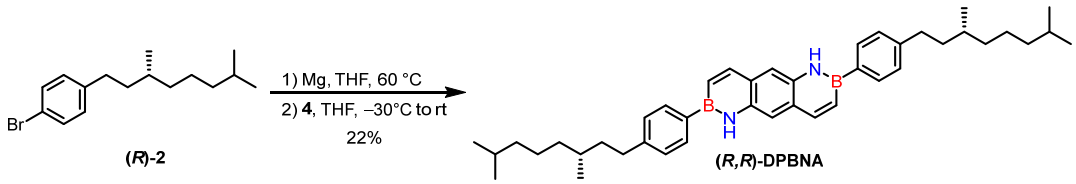

2,7-Bis(4-((*R*)-3,7-dimethyloctyl)phenyl)-1,2,6,7-tetrahydrobenzo[1,2-*e*:4,5-*e*']bis([1,2]azaborinine) ((*R,R*)-DPBNA). A solution of (*R*)-**2** (888 mg, 3.00 mmol) in 3 mL of THF under argon was added dropwise to a suspension of Mg (729 mg, 30.0 mmol) in 10 mL of THF at 60 °C. The mixture was refluxed at 60 °C for 2 h and then was cooled down to room temperature. The resulting Grignard reagent was added dropwise to a solution of compound **4** (206 mg, 0.831 mmol) in 10 mL of THF at –30 °C. The resulting mixture was allowed to warm to room temperature and stirred for 24 h. After completion of the reaction, the solvent was removed under reduced pressure, and the residue was purified by column chromatography over silica gel (eluent: petroleum ether/dichloromethane = 5 : 1) to give 112 mg (22%) of (*R,R*)-DPBNA as a white solid. ^{1}H NMR (400 MHz, $CDCl_3$, 298 K, ppm) δ 8.15 (d, J = 11.6 Hz, 2H), 8.10 (s, 2H), 7.86 (d, J = 7.6 Hz, 4H), 7.58 (s, 2H), 7.34-7.29 (m, 6H), 2.75-2.60 (m, 4H), 1.71-1.65 (m, 2H), 1.55-1.48 (m, 6H), 1.37-1.25 (m, 6H), 1.18-1.12 (m, 6H), 0.96 (d, J = 5.6 Hz, 6H), 0.88 (d, J = 6.8 Hz, 12H). ^{13}C NMR (101 MHz, $CDCl_3/CS_2$, 298 K, ppm) δ 144.79, 144.25, 134.98, 132.78, 128.40, 126.80, 116.76, 39.51, 39.00, 37.38, 33.78, 32.74, 28.20, 24.96, 22.86, 22.77, 19.77. HRMS (MALDI) *m/z*: Calcd. for $C_{42}H_{58}B_2N_2$: 612.4786; found: 612.4775 M^+.

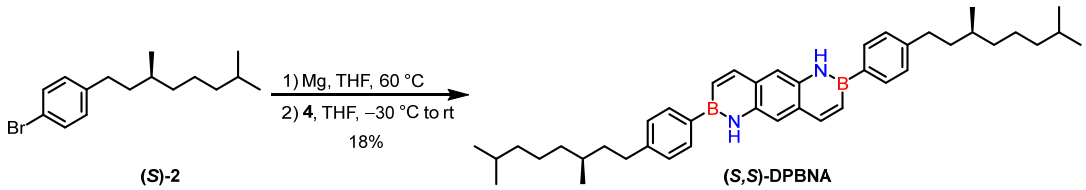

2,7-Bis(4-((*S*)-3,7-dimethyloctyl)phenyl)-1,2,6,7-tetrahydrobenzo[1,2-*e*:4,5-*e*']bis([1,2]azaborinine) (*S,S*)-DPBNA. Compound (*S*,*S*)-DPBNA was synthesized according to the same procedure as described above for the synthesis of (*R,R*)-DPBNA using (*S*)-**2** (1.04 g, 3.50 mmol), Mg (840 mg, 35.0 mmol), and **4** (248 mg, 1.00 mmol). After completion of the reaction, the solvent was removed under reduced pressure, and the residue was purified by column chromatography over silica gel (eluent: petroleum ether/dichloromethane = 5 : 1) to give 110 mg (18%) of (*S,S*)-DPBNA as a white solid. ^{1}H NMR (400 MHz, $CDCl_3$, 298 K, ppm) δ 8.16 (d, J = 11.6 Hz, 2H), 8.10 (s, 2H), 7.87 (d, J = 7.6 Hz, 4H), 7.58 (s, 2H), 7.34-7.29 (m, 6H), 2.75-2.60 (m, 4H), 1.71-1.65 (m, 2H), 1.55-1.49 (m, 6H), 1.37-1.25 (m, 6H), 1.18-1.12 (m, 6H), 0.96 (d, J = 6.0 Hz, 6H), 0.88 (d, J = 6.8, 12H). ^{13}C NMR (101 MHz, $CDCl_3/CS_2$, 298 K, ppm) δ 144.77, 144.24, 134.97, 132.78, 128.39, 126.79, 116.76, 39.51, 38.99, 37.38, 33.78, 32.74, 28.20, 24.96, 22.86, 22.77, 19.77. HRMS (MALDI) *m/z*: Calcd. for $C_{42}H_{58}B_2N_2$: 612.4786; found: 612.4785 M^+.

3. Device Fabrication and Characterization

Top-contact bottom-gate organic field-effect transistors (OFETs) with p-n heterojunction were fabricated as follows: (1) Silica wafers with a 300 nm-thick SiO_2 layer were sequentially washed with deionized water, acetone, and isopropanol, and then dried with a nitrogen flow and cleaned with plasma for 15 min at a high power. (2) The cleaned Si/SiO_2 substrates were modified with hexamethyldisilazane (HMDS) by spin-coating at 3000 rpm for 30 s, followed by thermal annealing at 100 °C for 30 min in a nitrogen-filled glove box. (3) Inspired by the quasi-planar heterojunction strategy used in organic solar cells,[4,5] we sequentially deposited F_4BDOPV-2T and (*S*,*S*)/(*R*,*R*)-DPBNA film on HMDS-modified Si/SiO_2 substrates to prepare p-n heterojunction. F_4BDOPV-2T polymer was dissolved at 5 mg mL^{-1} in 1,2-dichlorobenzene (*o*-DCB) at 120 °C for 8 h. (*S*,*S*)/(*R*,*R*)-DPBNA was dissolved at 3 mg mL^{-1} in chloroform (CF). Firstly, the F_4BDOPV-2T solution was spin-coated on the HMDS-modified Si/SiO_2 at 1500 rpm for 90 s, followed by annealing at 180 °C for 10 min and rapid cooling to room temperature. Next, the (*S*,*S*)- or (*R*,*R*)-DPBNA solution was

spin-coated onto the F_4BDOPV-2T film and annealed at 100 °C for 10 min. The slow dissolution process of F_4BDOPV-2T in organic solvents, which normally takes several hours at high temperatures,[6,7] and the rapid film-forming process of (*S*,*S*)/(*R*,*R*)-DPBNA in a low boiling-point solvent, ensured that the F_4BDOPV-2T film remained intact during spin-coating of (*S*,*S*)/(*R*,*R*)-DPBNA. Notably, samples for photophysical characterization were deposited on quartz substrates using the same preparation process. (4) Finally, 30 nm of Au was thermally evaporated on top of the (*S*,*S*)/(*R*,*R*)-DPBNA:F_4BDOPV-2T p-n heterojunction using shadow masks (length: 800 μm; width: 150 μm) as the source and drain electrodes.

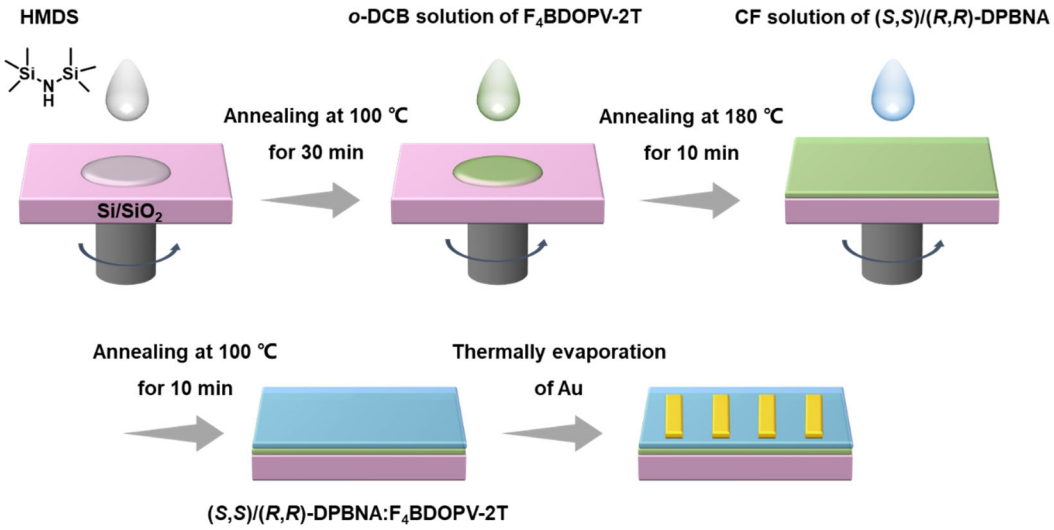

Fig. S1 The schematic diagram of preparing OFETs based on (*S*,*S*)/(*R*,*R*)-DPBNA:F_4BDOPV-2T p-n heterojunction.

The performance of OFETs and circularly polarized organic phototransistors (CP-OPTs) were measured at room temperature using an Agilent B1500A semiconductor parameter analyzer and an MPI TS150 probe station. Mobility was evaluated from the saturation region using the equation $I_{DS} = (W/2L)C_i\mu(V_G-V_T)^2$, where I_{DS} is the drain current, W is the channel width, L is the channel length, C_i is the capacitance of the insulating layer (300 nm SiO_2, 11 nF cm^{-2}), and V_G and V_T are the gate voltage and threshold voltage, respectively. Monochromatic light generated by a LED source (Microenerg Beijing Technology) was firstly transferred into linearly polarized light by a high-contrast UV linear polarizer (36-650, Edmund Optics) and then passed through a quarter-wave plate (AQWP05M-580, Thorlabs). By rotating the angle of quarter-wave plate, left-handed CPL (LCPL) and right-handed CPL (RCPL) were obtained. Prior to device testing, the purity of the CPL is

evaluated by transmitting it through a linear polarizer. The transmitted light intensity is measured while the polarizer is rotated. The intensity remains constant during the rotation, so the light is verified as pure CPL. Finally, the electrical and the photoresponsive performance of CP-OPTs were characterized in the dark and under the illumination of LCPL and RCPL at a wavelength of 365 nm. The light power density was measured using a Newport 843-R with Si photodetector.

4. Figures of Merit of CP-OPT

Key parameters of CP-OPTs, including photosensitivity (P), photoresponsivity (R), specific detectivity (D^*), and photocurrent dissymmetry factor (g_{ph}) were obtained from the transfer curves under dark and light irradiation. These parameters are crucial for evaluating the performance of CP-OPTs.

$$P = \frac{I_{ph}}{I_{dark}} = \frac{I_{light} - I_{dark}}{I_{dark}}$$

$$R = \frac{I_{light} - I_{dark}}{AP_{in}}$$

$$D^* = \frac{R\sqrt{A}}{\sqrt{2qI_{dark}}}$$

I_{light} is the drain current under light irradiation, I_{dark} is the drain current under dark, A is the effective light illumination area of the semiconductor layer, and P_{in} is the incident light power, q is the charge of an electron.

$$g_{ph} = \frac{2(I_{LCPL} - I_{RCPL})}{I_{LCPL} + I_{RCPL}}$$

I_{LCPL} is the drain current under LCPL irradiation, I_{RCPL} is the drain current under RCPL irradiation.

5. Photophysical and Electrochemical Properties

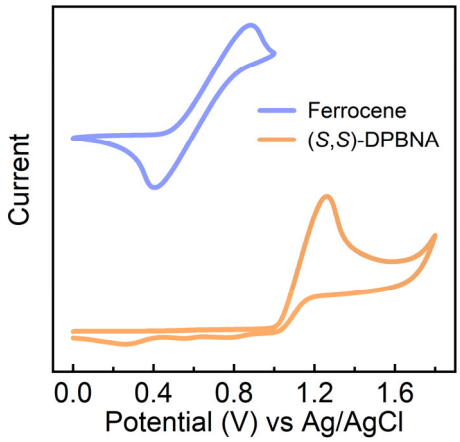

Fig. S2 CV curves of (*S*,*S*)-DPBNA in THF solution (1 mM) with 0.1 M *n*-Bu_4NPF_6 as supporting electrolyte and ferrocene as an external standard. Scan rate: 100 mV s^{-1}. The HOMO energy level is estimated from $E_{HOMO}^{sol} = -(4.80 + E_{ox}^{sol} - E_{Fc})$ based on the onset value and the LUMO energy level from $E_{LUMO}^{sol} = E_g^{opt,sol} + E_{HOMO}^{sol}$, $E_{Fc} = 0.51$ V.

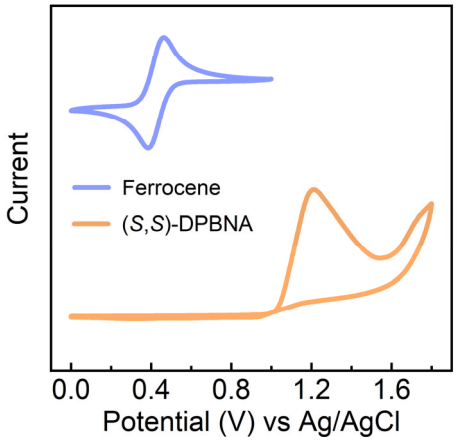

Fig. S3 CV curves of (*S*,*S*)-DPBNA film in acetonitrile with 0.1 M *n*-Bu_4NPF_6 as supporting electrolyte and ferrocene as an external standard. The (*S*,*S*)-DPBNA film was prepared by drop-casting a solution of (*S*,*S*)-DPBNA (2 mg mL^{-1} in CH_2Cl_2) on a glassy carbon electrode. Scan rate: 100 mV s^{-1}. The HOMO energy level is estimated from $E_{HOMO}^{film} = -(4.80 + E_{ox}^{film} - E_{Fc})$ based on the onset value and the LUMO energy level from $E_{LUMO}^{film} = E_g^{opt,film} + E_{HOMO}^{film}$, $E_{Fc} = 0.35$ V.

Table S1 Summary of the photophysical and electrochemical properties of (*S*,*S*)-DPBNA.

	λ_{onset}^{abs} (nm)	E_{gap}^{opt} (eV)	E_{ox} (V)	E_{HOMO} (eV)	E_{LUMO} (eV)
(*S*,*S*)-DPBNA^{sol}	412	3.01	1.03	–5.32	–2.31
(*S*,*S*)-DPBNA^{film}	424	2.92	1.03	–5.48	–2.56

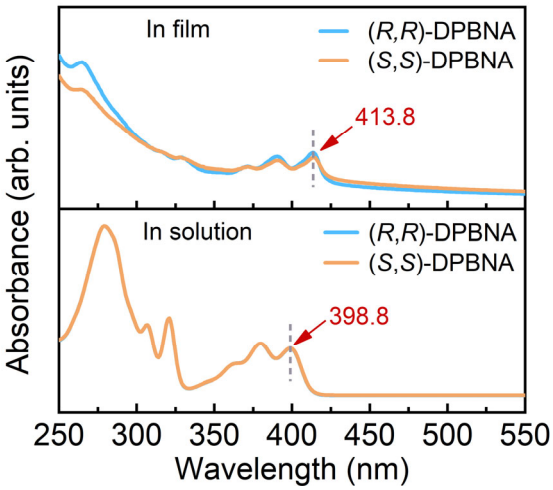

Fig. S4 UV-vis absorption spectra of (*S*,*S*)- and (*R*,*R*)-DPBNA in toluene solution and spin-coated film.

6. Thin-Film Morphologies

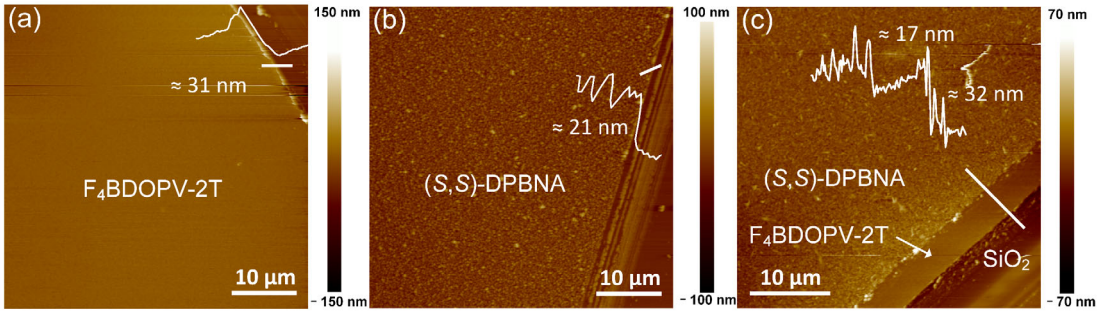

Fig. S5 AFM images of (a) the F_4BDOPV-2T polymer film, (b) the (*S*,*S*)-DPBNA film, and (c) the (*S*,*S*)-DPBNA:F_4BDOPV-2T p-n heterojunction.

7. Characterizations of UV CP-OPTs

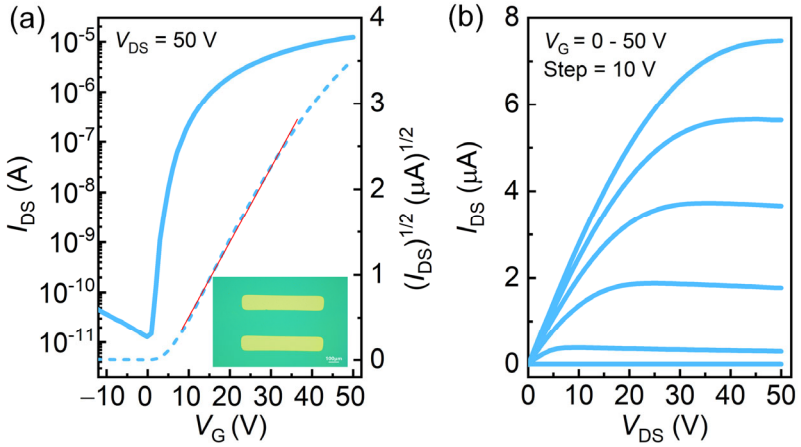

Fig. S6 Typical transfer (a) and output (b) characteristics of the (*R*,*R*)-DPBNA:F_4BDOPV-2T-based OFET. The electron mobility in the saturation regime is calculated from the slope obtained by linear fitting of $(I_{DS})^{1/2}$ and V_G in the range from 5 V to 36 V; slope = 8.70×10^{-5}, $W/L = 3.03$. The average electron mobility from five OFETs is 0.26 $cm^2\ V^{-1}\ s^{-1}$.

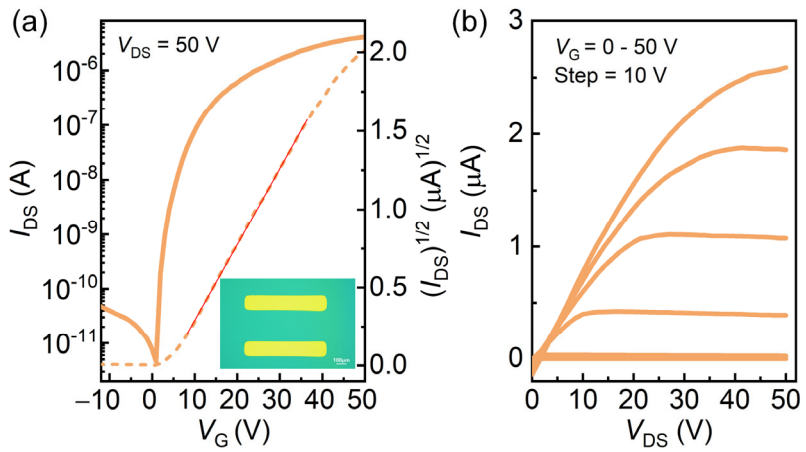

Fig. S7 Typical transfer (a) and output (b) characteristics of the (*S*,*S*)-DPBNA:F_4BDOPV-2T-based OFET. The electron mobility in the saturation regime is calculated from the slope obtained by linear fitting of $(I_{DS})^{1/2}$ and V_G in the range from 8 V to 36 V; slope = 4.85×10^{-5}, $W/L = 2.69$. The average electron mobility from five OFETs is 0.21 $cm^2\ V^{-1}\ s^{-1}$.

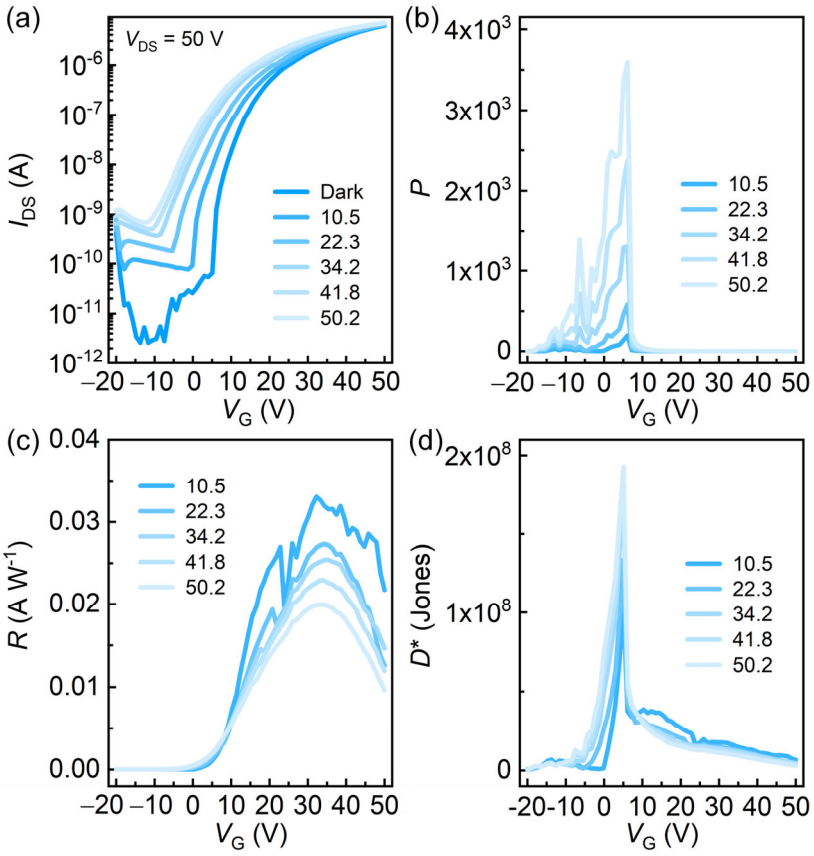

Fig. S8 (a) Transfer curves of (*R*,*R*)-DPBNA:F_4BDOPV-2T-based OPT under dark and different illumination intensities (λ = 365 nm, unit: mW cm^{-2}). (b-d) The *R*, *P*, and *D** as a function of V_G under different illumination intensities (unit: mW cm^{-2}).

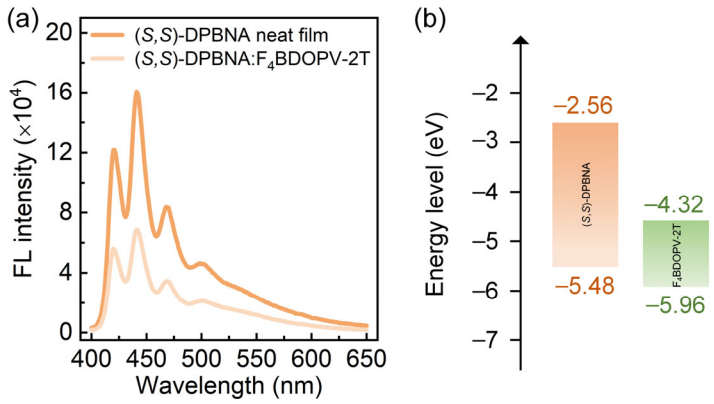

Fig. S9 (a) Fluorescence spectra of the (*S*,*S*)-DPBNA film and (*S*,*S*)-DPBNA:F_4BDOPV-2T p-n heterojunction at an excitation wavelength of 380 nm. (b) The energy level diagram of the (*S*,*S*)-DPBNA:F_4BDOPV-2T p-n heterojunction. The HOMO energy levels are estimated by CV measurements, and the LUMO levels are calculated based on the HOMO levels and the optical energy gaps in film. The data of F_4BDOPV-2T are taken from the literature.[7]

8. References

1. Gaussian 09, Revision D.01, M. J. Frisch, G. W. Trucks, H. B. Schlegel, G. E. Scuseria, M. A. Robb, J. R. Cheeseman, G. Scalmani, V. Barone, B. Mennucci, G. A. Petersson, H. Nakatsuji, M. Caricato, X. Li, H. P. Hratchian, A. F. Izmaylov, J. Bloino, G. Zheng, J. L. Sonnenberg, M. Hada, M. Ehara, K. Toyota, R. Fukuda, J. Hasegawa, M. Ishida, T. Nakajima, Y. Honda, O. Kitao, H. Nakai, T. Vreven, J. A. Montgomery, Jr., J. E. Peralta, F. Ogliaro, M. Bearpark, J. J. Heyd, E. Brothers, K. N. Kudin, V. N. Staroverov, T. Keith, R. Kobayashi, J. Normand, K. Raghavachari, A. Rendell, J. C. Burant, S. S. Iyengar, J. Tomasi, M. Cossi, N. Rega, J. M. Millam, M. Klene, J. E. Knox, J. B. Cross, V. Bakken, C. Adamo, J. Jaramillo, R. Gomperts, R. E. Stratmann, O. Yazyev, A. J. Austin, R. Cammi, C. Pomelli, J. W. Ochterski, R. L. Martin, K. Morokuma, V. G. Zakrzewski, G. A. Voth, P. Salvador, J. J. Dannenberg, S. Dapprich, A. D. Daniels, O. Farkas, J. B. Foresman, J. V. Ortiz, J. Cioslowski, and D. J. Fox, Gaussian, Inc., Wallingford CT, 2013.
2. J. S. Ishibashi, J. L. Marshall, A. Mazière, G. J. Lovinger, B. Li, L. N. Zakharov, A. Dargelos, A. Graciaa, A. Chrostowska and S.-Y. Liu, *J. Am. Chem. Soc.*, 2014, **136**, 15414-15421.
3. W. Li, C.-Z. Du, X.-Y. Chen, L. Fu, R.-R. Gao, Z.-F. Yao, J.-Y. Wang, W. Hu, J. Pei and X.-Y. Wang, *Angew. Chem. Int. Ed.*, 2022, **61**, e202201464.
4. H. W. C. Cao, D. Qiu, T. Zhao, Y. Zhu, X. Lai, M. Pu, Y. Li, H. Li, H. Chen, and F. He, *Adv. Funct. Mater.*, 2022, **32**, 2201828.
5. H. Chen, T. Zhao, L. Li, P. Tan, H. Lai, Y. Zhu, X. Lai, L. Han, N. Zheng, L. Guo and F. He, *Adv. Mater.*, 2021, **33**, 2102778.
6. Y.-Q. Zheng, Z.-F. Yao, T. Lei, J.-H. Dou, C.-Y. Yang, L. Zou, X. Meng, W. Ma, J.-Y. Wang and J. Pei, *Adv. Mater.*, 2017, **29**, 1701072.
7. Y.-Q. Zheng, T. Lei, J.-H. Dou, X. Xia, J.-Y. Wang, C.-J. Liu and J. Pei, *Adv. Mater.*, 2016, **28**, 7213-7219.

9. NMR and HRMS Spectra

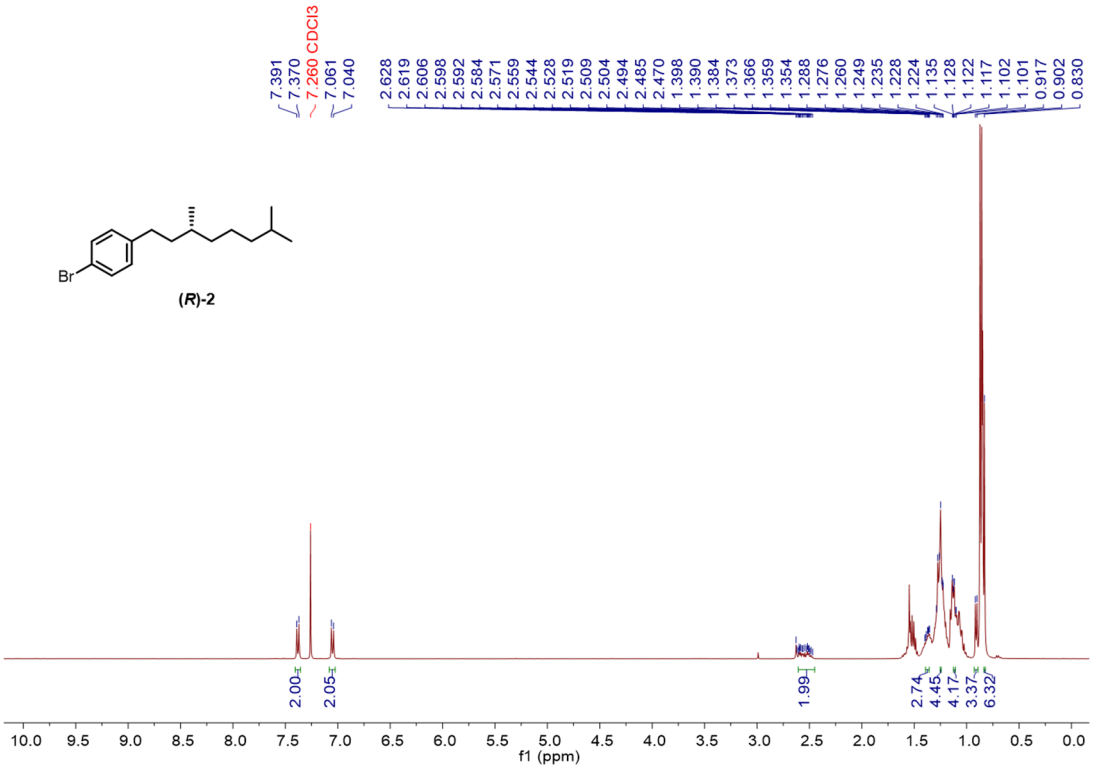

Fig. S10 ^{1}H NMR spectrum of compound (*R*)-**2** (400 MHz, $CDCl_3$, 298 K).

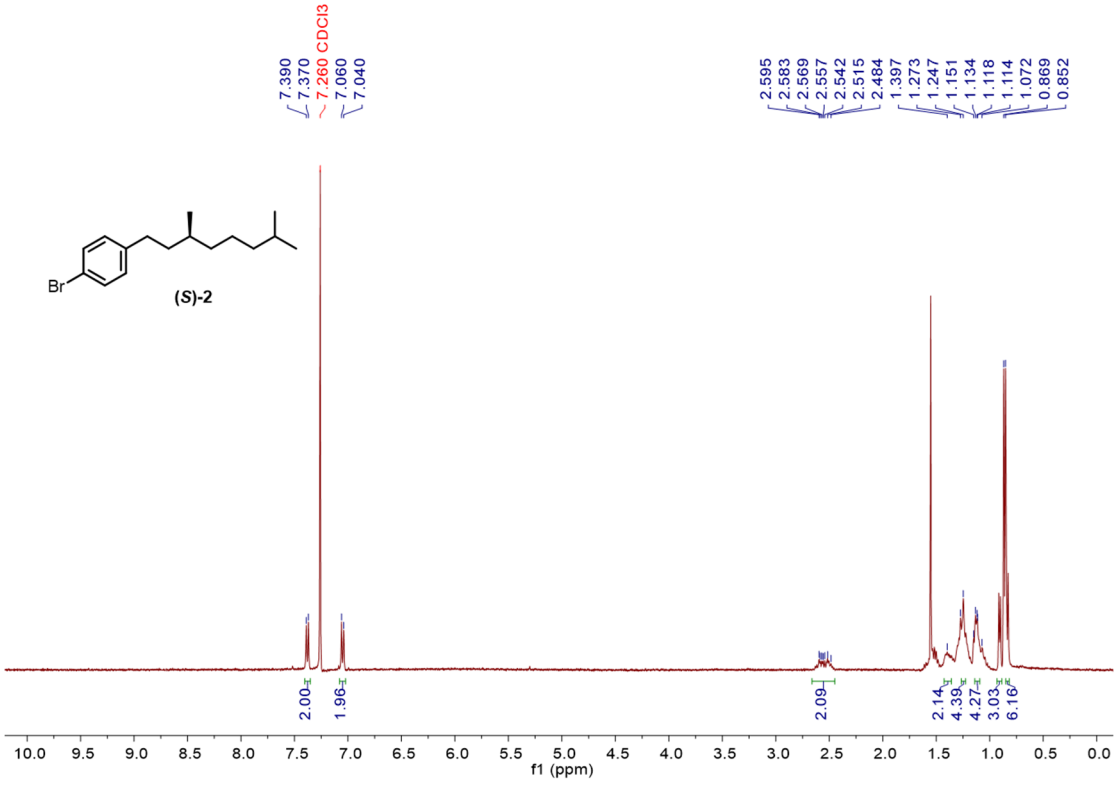

Fig. S11 ^{1}H NMR spectrum of compound (*S*)-**2** (400 MHz, $CDCl_3$, 298 K).

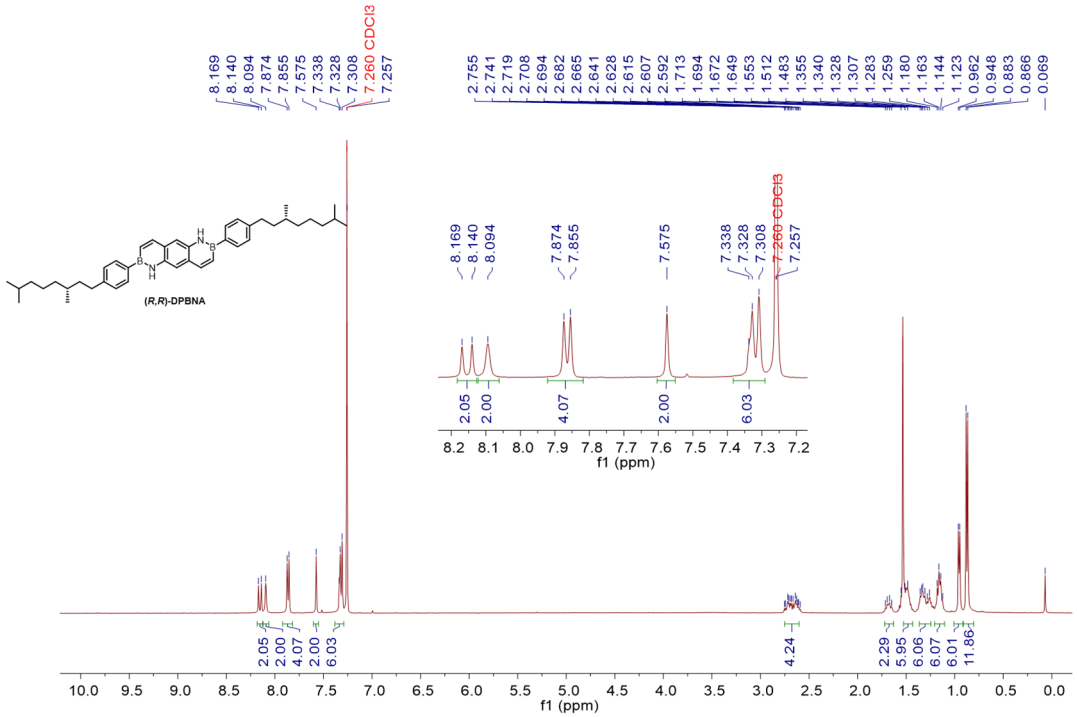

Fig. S12 ^{1}H NMR spectrum of (*R,R*)-DPBNA (400 MHz, $CDCl_3$, 298 K).

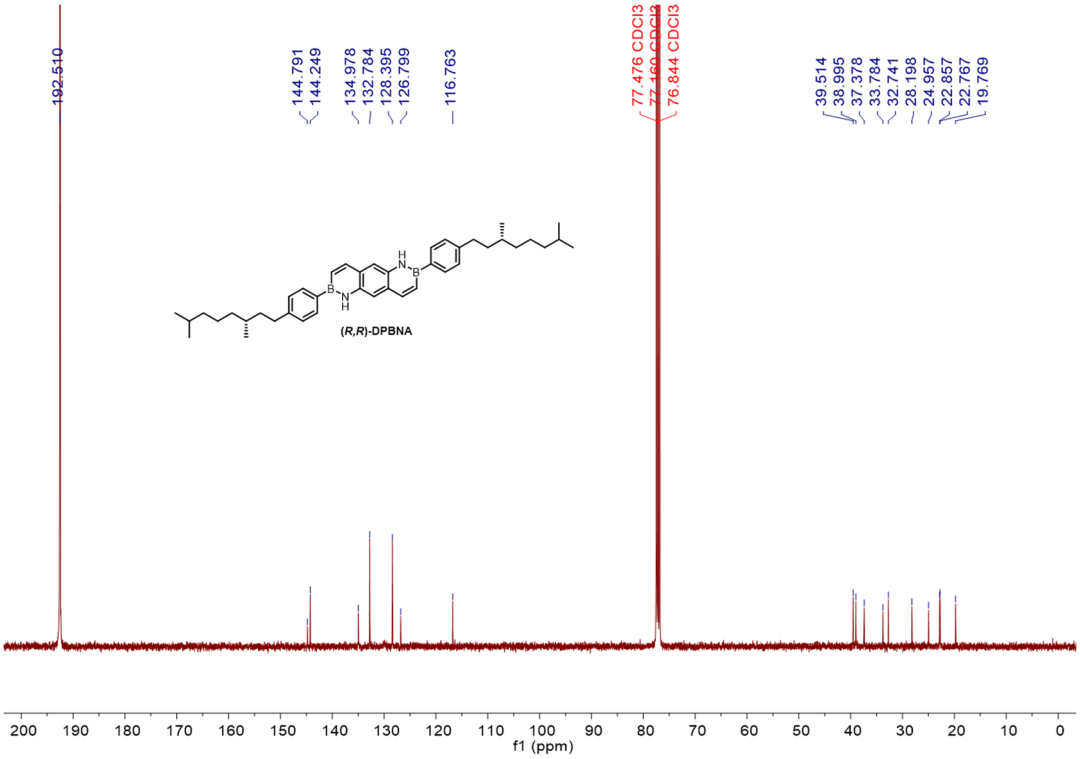

Fig. S13 ^{13}C NMR spectrum of (*R,R*)-DPBNA (101 MHz, $CDCl_3/CS_2$, 298 K).

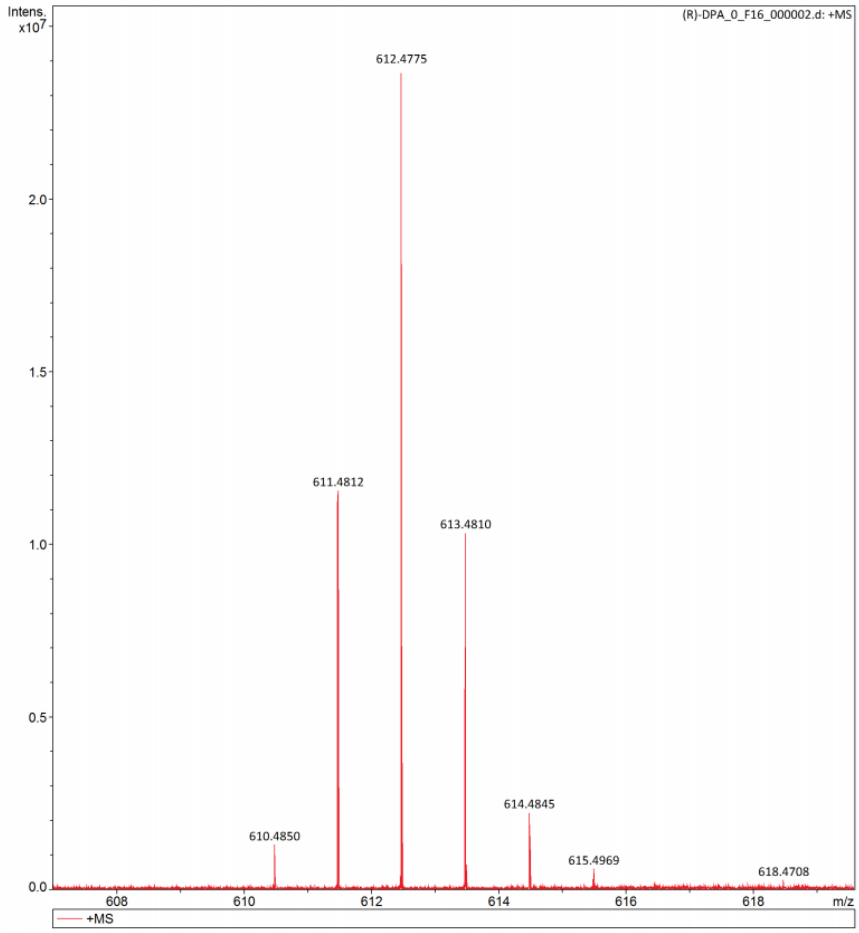

Fig. S14 High-resolution mass spectrometry (HRMS) spectrum of (*R,R*)-DPBNA.

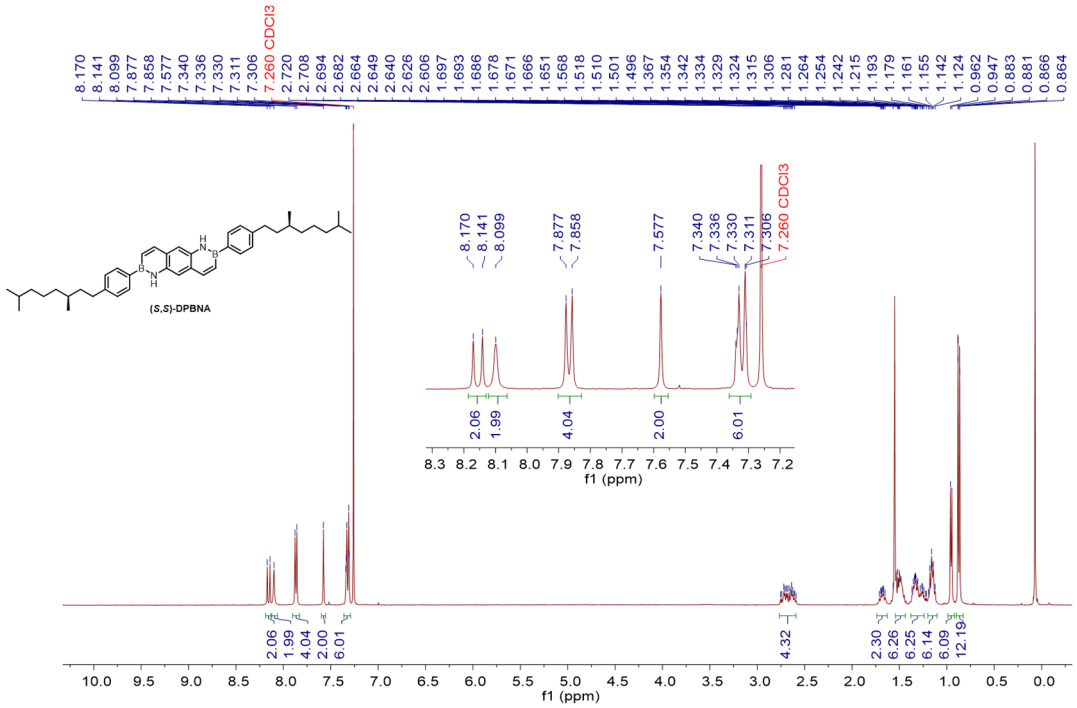

Fig. S15 ^{1}H NMR spectrum of (*S,S*)-DPBNA (400 MHz, $CDCl_3$, 298 K).

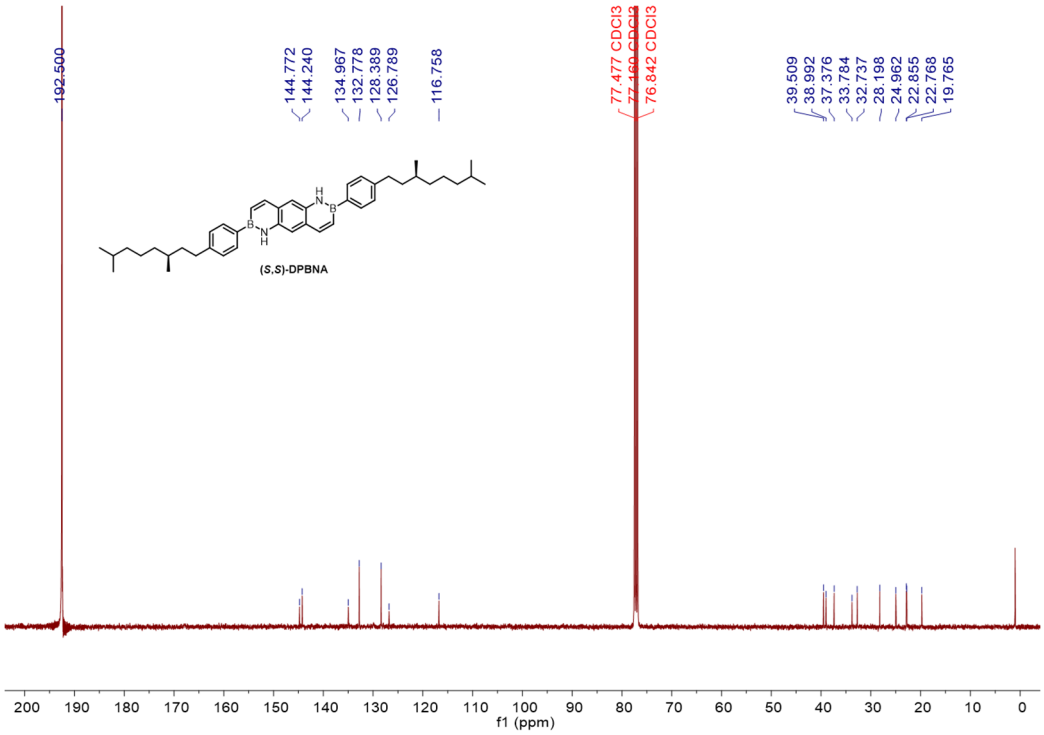

Fig. S16 ^{13}C NMR spectrum of (*S,S*)-DPBNA (101 MHz, $CDCl_3/CS_2$, 298 K).

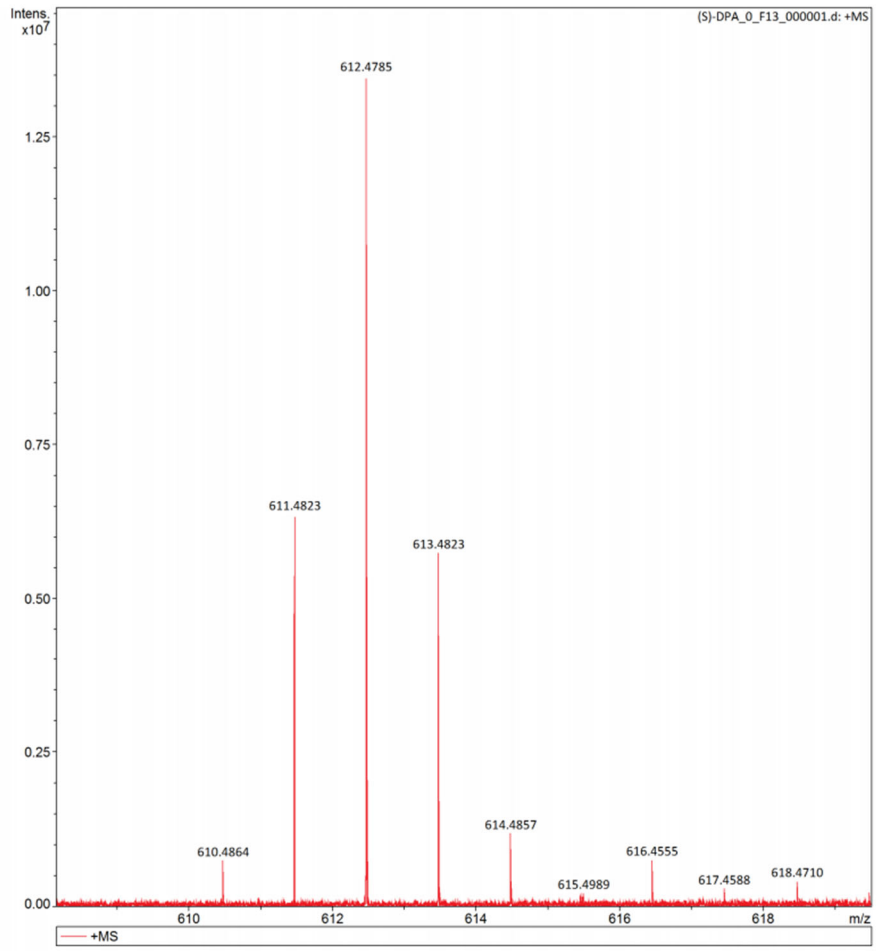

Fig. S17 High-resolution mass spectrometry (HRMS) spectrum of (*S,S*)-DPBNA.